Braiding and Fusion of Non-Abelian Vortex Anyons

T. Mawson,[1,*] T. C. Petersen,[1,2] J. K. Slingerland,[3,4] and T. P. Simula[1,5,†]

[1]*School of Physics and Astronomy, Monash University, Victoria 3800, Australia*
[2]*Monash Centre for Electron Microscopy, Monash University, Clayton 3800, Australia*
[3]*Department of Theoretical Physics, Maynooth University, County Kildare, Ireland*
[4]*Dublin Institute for Advanced Studies, School of Theoretical Physics, 10 Burlington Road, Dublin, Ireland*
[5]*Centre for Quantum and Optical Science, Swinburne University of Technology, Melbourne 3122, Australia*

We have studied topology and dynamics of quantum vortices in spin-2 Bose-Einstein condensates. By computationally modeling controllable braiding and fusion of these vortices, we have demonstrated that certain vortices in such spinor condensates behave as non-Abelian anyons. We identify these anyons as fluxon, chargeon, and dyon quasiparticles. The pertinent anyon models are defined by the quantum double of the underlying discrete non-Abelian symmetry group of the condensate ground state order parameter.

All elementary particles are classified by their quantum statistics as either bosons or fermions. However, in certain two-dimensional materials, particlelike excitations—anyons—which are neither bosons nor fermions, have been predicted to emerge [1,2]. When two anyons are exchanged, braiding their space-time world lines, the system's wave function may accumulate an arbitrary phase not restricted to the specific values corresponding to bosons or fermions. For non-Abelian anyons, exchange may act through noncommuting unitary operators, rather than simple phases. Also, how such anyons fuse (combine) when brought together depends on the history of their paths prior to the fusion. Encoding information in the nonlocal fusion properties of non-Abelian anyons forms a tantalizing prospect for realization of a fault-tolerant universal quantum computer [3,4].

Recent advances in quantum computing have come from intense research focus on qubits realized in a variety of systems including trapped ions [5–7], spins in silicon atoms [8,9], and superconducting circuits [10,11]. Such systems must contend with the accumulation of spontaneous errors due to the interactions with the environment. In contrast, topological quantum computers based on topological qubits made of non-Abelian anyons are anticipated to be more resilient due to being topologically protected from many conventional types of decoherence. Two promising non-Abelian anyon platforms are the Fibonacci and Ising anyon models [12–16]. A number of experiments have explored the potential realization of such anyons in condensed matter systems including Majorana zero modes [17–21] and quasiparticles in certain fractional quantum Hall states [22–24]. Other non-Abelian anyon models have been proposed to be realizable using fluxons [25–27]. Notwithstanding, the existence of a physical system of non-Abelian anyons capable of universal quantum computation remains an open question.

Theoretically, it is known that quantum vortices in superfluids are capable of accommodating non-Abelian quasiparticles. Both Fermi gases with putative chiral *p*-wave order parameter and fermionic superfluid helium 3, if confined in two dimensions, have been predicted to host Majorana zero modes trapped by their vortex cores [28–33]. Furthermore, in certain high-spin Bose gases, such as those considered in this Letter, vortices are characterized by non-Abelian symmetry groups [34–38], that result in nontrivial topological interactions between vortices [39].

Here, we build upon these ideas by performing direct numerical simulations of controllable braiding and fusion of non-Abelian vortices in spinor Bose gases. We computationally demonstrate that certain fractional vortices—particlelike topological excitations in two-dimensional (2D) spinor Bose-Einstein condensates (BECs)—may be non-Abelian fluxon anyons and are potentially useful for applications in topological quantum information processing and storage. In addition to fluxons, excitations in these systems include chargeons [40] and charge-flux composites known as dyons [41–44]. The full spectrum of excitations is labeled using the quantum double of the symmetry group of the condensate [45]. In addition to chargeons, these systems also allow for completely delocalized Cheshire charges [46,47]. We simulate the braiding and fusion of non-Abelian vortex anyons by employing external pinning potentials that could be realized using focused laser beams [48,49], to controllably manipulate the states of topological qubits constructed from such non-Abelian vortex anyons.

Non-Abelian vortex anyons.—A non-Abelian anyon model has three essential aspects: (i) a list of particle types, (ii) a set of fusion rules that determine the types of particles formed after fusing together two particles, and (iii) braiding rules that describe the effect of exchanging the

positions of two particles. We demonstrate that the topological interactions of our non-Abelian fractional vortices in spinor Bose-Einstein condensates [35–37,50–54] contain the essential aspects of a non-Abelian anyon model. The anyon models involved are similar to those of non-Abelian toric code models [4] or discrete gauge theories [45].

Physically, the order parameter of a spinor BEC inherits a spin degree of freedom from the spin of the atoms. Interactions between atoms then select out, in general, a non-Abelian stabilizer subgroup H of symmetries which leaves the condensate ground state order parameter locally invariant. Vortices are labeled by elements of H, which we call fluxes. Vortices with noncommuting topological fluxes are called non-Abelian and are characterized by nontrivial, path dependent, topological interactions.

Specifically, we consider a spin-2 Bose-Einstein condensate in a box trap in zero external magnetic field with the particle interaction strengths chosen to realize the cyclic-tetrahedral superfluid ground state phase, for which H is the non-Abelian binary tetrahedral symmetry group [55].

Figure 1 shows the outcome of a numerical experiment, obtained by solving the spin-2 Gross-Pitaevskii equation (see Supplemental Material [55]) in 2D governed by a five component spinor wave function Ψ, that demonstrates the exotic braiding and fusion dynamics of non-Abelian vortices. The system is initialized at time $t = 0$ in Fig. 1(a) by creating four non-Abelian vortices in the Bose-Einstein condensate by phase imprinting two vortex-antivortex pairs [55]. Using pinning potentials that model an array of Gaussian-shaped laser beams that repel atoms, the vortices can be pinned and controllably moved around, forming a braid in their space-time world lines as shown in Fig. 1(a) [55]. A plat closure of the braid is realized by the initial pair creation and final fusion of the vortex pairs. The effects of braiding the vortices are observed at different dimensionless times $\tilde{t} = t\omega$, where $\omega = 2\pi \times 5$ Hz, after, alternatively, (i) releasing the pinning potentials and measuring the properties of the four vortices, see lower rows in Figs. 1(b)–1(f), or, (ii) fusing the two vortex pairs first and then measuring the result after releasing the pinning potentials, see upper rows in Figs. 1(b)–1(f). The vortex locations are visualized via their core structure, which may have nonzero spin-singlet pair amplitude, $|A|^2$, and/or nonzero magnetization, F_z [55].

A detailed understanding of the observed dynamics comes from labeling the flux of each vortex in Figs. 1(b)–1(f), enabled by the vortex identification method described in Ref. [54]. Briefly, at any moment in time, we are able to interrogate the complete spinor wave function numerically and, thus, measure a generalized geometric phase along any closed path surrounding a vortex or multiple vortices [54]. Such a measurement will reveal the enclosed net flux and can be used for determining the outcomes of braidings and fusions.
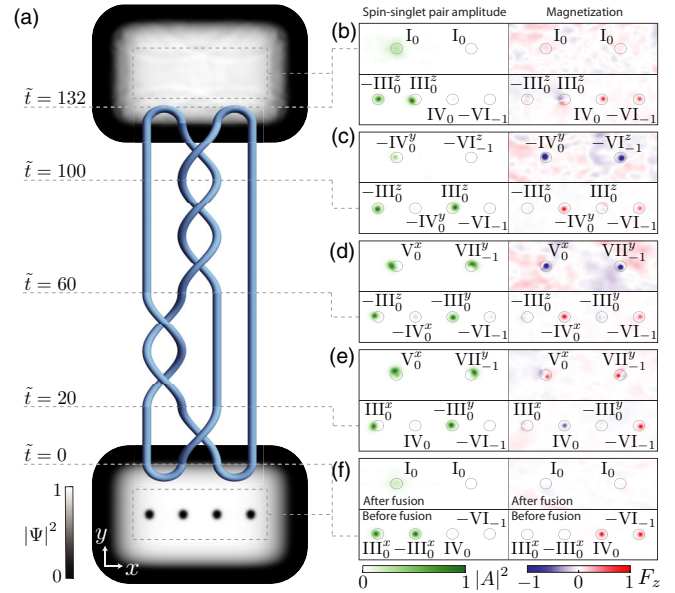

FIG. 1. Braiding and fusion of non-Abelian fractional vortices. (a) The paths of vortices embedded in a two-dimensional Bose-Einstein condensate trace out world lines that form a braid whose plat closure yields a link. The total condensate density is shown for the initial ($\tilde{t} = 0$) and final ($\tilde{t} = 132$) states. (b) Spin-singlet pair amplitude (left column) and magnetization (right column) with vortex locations marked using circles and labeled by the vortex (anyon) types. The upper rows correspond to the system state just after the vortices have been fused pairwise and the lower rows correspond to the state just before the fusion. The field of view of each of the four frames in (b)–(f) corresponds to the dashed rectangle shown in (a) where the intervortex separation is 27 μm. The dimensionless times $\tilde{t} = t\omega$ of measurement of states (b)–(f) are marked in (a).

The vortex labels have the form $\pm X_\eta^\nu$, where X_η is a Roman numeral denoting the fluxon part of the anyon type. The state of each anyon is characterized by one of several (conjugate) fluxes specified by the internal quantum numbers ν and η, and the $\pm$ sign [55]. Underpinning the braiding dynamics is the long-range topological influence between non-Abelian vortices [26,27,39]. For an anticlockwise elementary braid (exchange of a pair) of vortices with fluxes (γ_1, γ_2) their mutual topological influence converts their fluxes to $(\gamma_2, \gamma_2\gamma_1\gamma_2^{-1})$, [55]. The products and the inverse in $\gamma_2\gamma_1\gamma_2^{-1}$ are taken in the stabilizer group H [55]. If γ_1 and γ_2 do not commute, this mapping permutes the flux of the second vortex within the set of fluxes associated with its anyon type. The clockwise exchange realises the map $(\gamma_1, \gamma_2) \rightarrow (\gamma_1^{-1}\gamma_2\gamma_1, \gamma_1)$. Braiding may also enact a local unitary transformation on the wave function, which reverses the sign of the vortex core magnetization, turning a red core into a blue core, and vice versa, without changing the value of their fluxes, as shown in Figs. 1(e) and 1(d). The outcome of fusing two vortices is determined by an ordered product of their two fluxes equivalent to their total flux. Only vortices whose fluxes multiply to the identity

element of H may annihilate, otherwise, the fusion results in a remnant vortex. It is also possible for vortices with commuting fluxes to pass through each other without apparent interaction [25,54].

The initial vortex-antivortex pairs in Fig. 1(f) (lower row) consist of three particle types: two vortices of the same type (III_0) with nonzero $|A|^2$, green cores, and two of different types (IV_0 and VI_{-1}) with $F_z > 0$, red cores. Initially, both pairs annihilate upon being fused [Fig. 1(f), upper row], by construction. An exchange of the two vortices in the middle leads to the state measured at $\tilde{t} = 20$, shown in Fig. 1(e). The braid swaps the positions of two vortices, which trivially changes the pairwise fusion dynamics as neither the green and red nor green and blue cored vortices can annihilate. The braid between $\tilde{t} = 60$ and $\tilde{t} = 100$ consists of two exchanges (elementary braids) of the two middle vortices resulting in the state shown in Fig. 1(c). Importantly, although this braiding preserves the ordering of the vortex types by returning them to their original prebraiding positions at $\tilde{t} = 60$, the types of vortices formed after fusion are different before (V_0 and VII_{-1} at $\tilde{t} = 60$) and after (IV_0 and VI_{-1} at $\tilde{t} = 100$) the braiding. Such vortex metamorphosis due to braiding is a hallmark of non-Abelian anyons. The final exchange of the middle two vortices results in the state at $\tilde{t} = 132$, shown in Fig. 1(b), where the two non-Abelian vortex anyon pairs again annihilate.

Vortex anyon model.—The cyclic-tetrahedral phase of a spin-2 BEC supports seven distinct fluxon types, labeled as I_η–VII_η [55]. Each of the seven types of fluxon comes with several possible charge labels and, taking these into account, we obtain the fusion and braiding rules for a complete anyon model. Here, we will focus mostly on the fusion of the flux types. The fusion outcomes of the lowest energy fluxons are detailed in the table presented in the Supplemental Material, Fig. S2 [55]. Although types IV_η–VII_η vortices are non-Abelian anyons, their fusion rules do not preserve the winding number η of the anyons, complicating their potential use for topological quantum computation. However, restricting to the set of three fluxons I_0, II_0, and III_0, hereafter, referred to as $\mathbf{1}$, σ, and τ, respectively, results in a concise non-Abelian anyon model. The fusion of two chargeless τ anyons may result in either a 1, σ, or τ anyon, with the explicit fusion rule $\tau \otimes \tau = N_{\tau\tau}^{\mathbf{1}}\mathbf{1} \oplus N_{\tau\tau}^{\sigma}\sigma \oplus N_{\tau\tau}^{\tau}\tau$, where the multipliers $N_{\tau\tau}^{\mathbf{1}} = 6$, $N_{\tau\tau}^{\sigma} = 6$, and $N_{\tau\tau}^{\tau} = 4$ mean that when anyons a and b fuse, they may form a c anyon in N_{ab}^c distinct ways [55]. Note that the six distinguishable ways the τ fluxons can fuse to the flux vacuum are further split by the four possible resulting Cheshire charge states, and that only one of those six fusion channels corresponds to the true vacuum state having both vanishing flux and charge [55]. The non-Abelian τ anyon is its own antiparticle such that, upon fusion, two τ anyons may annihilate each other. The remaining flux fusion rules of this anyon model are; $\tau \otimes \sigma = \tau$, $\sigma \otimes \sigma = \mathbf{1}$, and $x \otimes \mathbf{1} = x$, where

$x \in \{\mathbf{1}, \sigma, \tau\}$. The anyons 1 and σ are Abelian with quantum dimensions $d_{\mathbf{1}} = d_{\sigma} = 1$, respectively. The τ anyon is the non-Abelian (fluxon) anyon of the theory with a quantum dimension, $d_{\tau} = 6$, larger than both the Fibonacci and Ising anyon models.

Topological qubits.—The different fusion outcomes of the anyons define a fusion path, equivalent to a set of topologically distinct states, which can be used for encoding quantum information. We are inspired by the Fibonacci anyon model where the fusion of three anyons allows a topological qubit to be defined as a two-level system plus one noncomputational state. In the case of three τ fluxons, the number of distinct fusion paths in which information could be stored is significantly larger than in the Fibonacci anyon model. Nevertheless, for the sake of demonstration, we consider braiding operations with three fluxons that involve only a subset of the many states in the full fusion space and, therefore, may be conveniently discussed in terms of effective qubits. A natural choice for the zero state corresponds to the creation of two pairs of τ fluxons from the true vacuum. The rightmost of the four anyons will not be part of the qubit and will not take part in any braiding processes we consider. The zero state of the qubit is, then, $|0\rangle = \frac{1}{6}\sum_{\gamma_1,\gamma_2 \in \mathrm{III}} |\gamma_1, \gamma_1^{-1}, \gamma_2\rangle$, corresponding to three τ anyons with fluxes γ_1, γ_1^{-1}, and γ_2, respectively. A convenient choice for the second qubit state is $|1\rangle = \frac{1}{6}\sum_{\gamma_1,\gamma_2 \in \mathrm{III}} |\gamma_1, \gamma_1, \gamma_2\rangle$, corresponding to the fusion of the τ fluxon pair to the σ fluxon.

Figure 2 demonstrates the action of manipulating the state of such a topological qubit by controllable braiding of the anyons. Initially, the fluxons are prepared in the $|0\rangle$ state, which, in practice, could be achieved by nucleating two vortex-antivortex pairs that introduces a fourth, surplus, anyon which is disregarded in this numerical experiment without consequence.

A unitary operation, encoded by the braid in Fig. 2(a), is applied to the fluxons by moving the pinning potentials to exchange the second and third anyons within the qubit structure twice. Once the braiding has been completed, a measurement of the state is made by fusing the first and second anyons from the left of the condensate and observing the remaining core structures shortly after the pinning potentials have been withdrawn. Prior to the fusion, the three τ anyons are identified by the green $|A|^2$ cores, as shown in Fig. 2(b). After the braiding, the measurement outcome depends on the topological influence between the exchanged anyons. The braid maps the $|0\rangle$ state to a superposition

$$\sum_{\substack{\gamma_1,\gamma_2 \in \mathrm{III} \\ \gamma_1\gamma_2 = \gamma_2\gamma_1}} \frac{|\gamma_1, \gamma_1^{-1}, \gamma_2\rangle}{2\sqrt{3}} + \sum_{\substack{\gamma_1,\gamma_2 \in \mathrm{III} \\ \gamma_1\gamma_2 \neq \gamma_2\gamma_1}} \frac{|\gamma_1, \gamma_1, \gamma_2\rangle}{2\sqrt{6}}, \quad (1)$$

where the two sums contain the combinations of fluxes which braided with trivial and nontrivial topological influence, respectively. The probability p that a measurement would
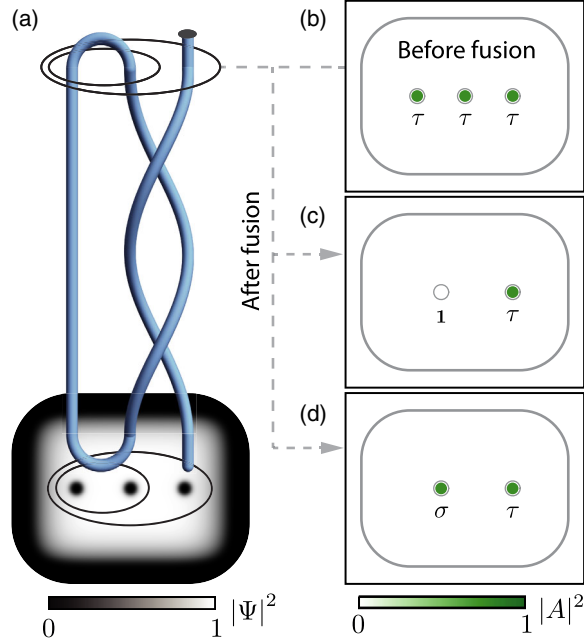
FIG. 2. Single qubit braiding operation. (a) The paths of the three τ anyons trace out braided world lines enacting a unitary operation on the initial state. Time flows upward. The total condensate density is shown for the initial state. The overlayed concentric ellipses denote the orientation of the qubit as a graphical representation of the bracket notation used in the text. (b) Spin-singlet pair amplitude of the qubit just before the fusion. The rounded rectangle marks the boundary of the condensate, and the vortex locations are denoted by the circles, the intervortex separation is 27 μm. (c) A fusion outcome corresponding to the annihilation of the first two anyons as in the $|0\rangle$ state [55]. (d) A fusion outcome corresponding to the nonannihilation of the first two anyons as in the $|1\rangle$ state [55]. Data in (b)–(d) are thresholded relative to half the maximum value in (b) and any maxima within the vortex location markers are mapped to the solid green circles [55]. The specific fluxes of the three initial state vortices in (c) are $(III_0^x, -III_0^x, III_0^x)$, and in (d), they are $(III_0^x, -III_0^x, III_0^y)$.

record complete annihilation $p(0) = 1/3$ or the formation of a σ fluxon $p(1) = 2/3$ after the braiding is obtained by projecting the braided superposition state onto the two qubit basis states $|0\rangle$ and $|1\rangle$. Prior to the fusion measurement, the two possibilities are indistinguishable by any local observation. In general, braiding, with respect to this basis, would introduce significant leakage into the noncomputational fusion paths even for the case of a single qubit. However, this is not a real problem as we only restricted to a two dimensional space for illustrative purposes. Any realistic implementation would use the full fusion space for computations.

In the numerical experiments, we simulate two specific components of the $|0\rangle$ state, those with fluxes $(III_0^x, -III_0^x, III_0^x)$ and $(III_0^x, -III_0^x, III_0^y)$, such that the braid acts on these basis states in a deterministic manner. In the first case, the exchanged anyons commute so the braid realizes a trivial topological influence, and the fusion
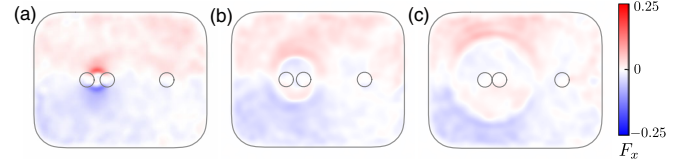

FIG. 3. Signatures of a Cheshire charge. Frames (a)–(c) show the x component of the magnetization density of the condensate at the end of the simulation of Fig. 2(c). The time interval between the frames is $\delta t \approx 16$ ms. The circular markers denote the locations of the vortex pinning sites. The expanding ring shaped magnetic soliton structure is emitted due to the fusion of two fluxons [55].

measures the $|0\rangle$ state, shown in Fig. 2(c), characterized by a single green core. However, in the latter case, they do not commute so the nontrivial topological influence changes the signs of the anyons, and the fusion measures the state $|1\rangle$ of the topological qubit. Such a measurement of the $|1\rangle$ state is illustrated in Fig. 2(d) and corresponds to the observation of two green vortex cores, with the additional filled core corresponding to a σ anyon formed in the fusion of the two τ anyons.

If spurious vortex-antivortex pairs were nucleated during the braiding process, they could, in principle, braid with the system vortices leading to topological decoherence via quasiparticle poisoning [15]. Consequently, the fusion outcomes could no longer be uniquely identified by the simple green or no green blob signal illustrated in Fig. 2 [55]. However, this does not occur in our adiabatic zero-temperature braiding simulations and we numerically measure the fluxes of the vortices explicitly to verify that the simple blob measurement, indeed, faithfully identifies the fusion outcomes in these simulations.

Cheshire charge.—We have discussed the topological qubit at the fluxon level, ignoring the chargeons. However, the states considered in the single qubit simulations are τ flux eigenstates, which correspond to charge superposition states. Here, the charge arises as Cheshire charge [46,47,76], which may be revealed when the vortices are annihilated causing the delocalized Cheshire charge to appear. After a Cheshire charge localizes to a chargeon, it could reform as a pair of Alice vortices or a propagating Alice ring [47]. In our single qubit simulations, we have observed a propagating ring-shaped soliton structure in the magnetization density of the condensate, Figs. 3(a)–3(c) [55]. This observed signature may be related to the phenomenology of Cheshire charges.

Anyons based on finite groups that are solvable but not nilpotent are capable of universal quantum computation [77]. Since the binary tetrahedral group does satisfy these criteria, it may be a fruitful platform for developing a universal quantum computer. A method for generating multiple non-Abelian vortices has been outlined in [53]. However, to realize such vortices experimentally, a series of engineering challenges must be confronted [55]. To ensure the non-Abelian topology, our numerical experiments employ spin

interaction strengths which are not currently achievable in experiment. However, a recent proposal by Hurst and Spielman, Ref. [78], may provide an experimentally realizable pathway for effectively tuning the spin interactions. Promisingly, many additional non-Abelian phases have been predicted for higher spin BEC systems [38], which may enable a more accessible experimental route for creating non-Abelian vortex anyons. To surpass the inertial limitations of massive vortices [79], including the adiabaticity speed limit of vortex braiding [80], synthetic non-Abelian fluxons could potentially be designed and engineered using novel artificial gauge field techniques [81,82]. The ability to perform quantum information processing with the non-Abelian vortices may be compromised by the substantial challenge of creating and maintaining true quantum superpositions with a macroscopic number of atoms in a Bose-Einstein condensate. However, we conclude that non-Abelian vortices in spinor Bose-Einstein condensates hold promise for a tangible demonstration of the underlying principles of topological quantum computation and should be pursued further.

*Corresponding author.
thomas.mawson@monash.edu
†Corresponding author.
tsimula@swin.edu.au

[1] J. M. Leinaas and J. Myrheim, Nuovo Cimento B **37**, 1 (1977).
[2] F. Wilczek, Phys. Rev. Lett. **48**, 1144 (1982).
[3] M. H. Freedman, Proc. Natl. Acad. Sci. U.S.A. **95**, 98 (1998).
[4] A. Y. Kitaev, Ann. Phys. (Amsterdam) **303**, 2 (2003).
[5] J. I. Cirac and P. Zoller, Phys. Rev. Lett. **74**, 4091 (1995).
[6] C. Ospelkaus, U. Warring, Y. Colombe, K. R. Brown, J. M. Amini, D. Leibfried, and D. J. Wineland, Nature (London) **476**, 181 (2011).
[7] D. Nigg, M. Müller, E. A. Martinez, P. Schindler, M. Hennrich, T. Monz, M. A. Martin-Delgado, and R. Blatt, Science **345**, 302 (2014).
[8] F. A. Zwanenburg, A. S. Dzurak, A. Morello, M. Y. Simmons, L. C. L. Hollenberg, G. Klimeck, S. Rogge, S. N. Coppersmith, and M. A. Eriksson, Rev. Mod. Phys. **85**, 961 (2013).
[9] T. F. Watson, S. G. J. Philips, E. Kawakami, D. R. Ward, P. Scarlino, M. Veldhorst, D. E. Savage, M. G. Lagally, M. Friesen, S. N. Coppersmith, M. A. Eriksson, and L. M. K. Vandersypen, Nature (London) **555**, 633 (2018).
[10] J. Clarke and F. K. Wilhelm, Nature (London) **453**, 1031 (2008).
[11] G. Wendin, Rep. Prog. Phys. **80**, 106001 (2017).
[12] A. Kitaev, Ann. Phys. (Amsterdam) **321**, 2 (2006).
[13] S. Trebst, M. Troyer, Z. Wang, and A. W. W. Ludwig, Prog. Theor. Phys. Suppl. **176**, 384 (2008).
[14] C. Nayak, S. H. Simon, A. Stern, M. Freedman, and S. Das Sarma, Rev. Mod. Phys. **80**, 1083 (2008).
[15] S. Das Sarma, M. Freedman, and C. Nayak, npj Quantum Inf. **1**, 15001 (2015).
[16] B. Field and T. Simula, Quantum Sci. Technol. **3**, 045004 (2018).
[17] V. Mourik, K. Zuo, S. M. Frolov, S. R. Plissard, E. P. A. M. Bakkers, and L. P. Kouwenhoven, Science **336**, 1003 (2012).
[18] S. Nadj-Perge, I. K. Drozdov, J. Li, H. Chen, S. Jeon, J. Seo, A. H. MacDonald, B. A. Bernevig, and A. Yazdani, Science **346**, 602 (2014).
[19] Q. L. He, L. Pan, A. L. Stern, E. C. Burks, X. Che, G. Yin, J. Wang, B. Lian, Q. Zhou, E. S. Choi, K. Murata, X. Kou, Z. Chen, T. Nie, Q. Shao, Y. Fan, S.-C. Zhang, K. Liu, J. Xia, and K. L. Wang, Science **357**, 294 (2017).
[20] H. Zhang *et al.*, Nature (London) **556**, 74 (2018).
[21] P. Zhang, K. Yaji, T. Hashimoto, Y. Ota, T. Kondo, K. Okazaki, Z. Wang, J. Wen, G. D. Gu, H. Ding, and S. Shin, Science **360**, 182 (2018).
[22] I. P. Radu, J. B. Miller, C. M. Marcus, M. A. Kastner, L. N. Pfeiffer, and K. W. West, Science **320**, 899 (2008).
[23] M. Dolev, M. Heiblum, V. Umansky, A. Stern, and D. Mahalu, Nature (London) **452**, 829 (2008).
[24] R. L. Willett, L. N. Pfeiffer, and K. W. West, Proc. Natl. Acad. Sci. U.S.A. **106**, 8853 (2009).
[25] F. A. Bais, Nucl. Phys. **B170**, 32 (1980).
[26] L. Brekke, H. Dykstra, A. F. Falk, and T. D. Imbo, Phys. Lett. B **304**, 127 (1993).
[27] H.-K. Lo and J. Preskill, Phys. Rev. D **48**, 4821 (1993).
[28] N. B. Kopnin and M. M. Salomaa, Phys. Rev. B **44**, 9667 (1991).
[29] G. E. Volovik, J. Exp. Theor. Phys. Lett. **70**, 609 (1999).
[30] S. Tewari, S. Das Sarma, C. Nayak, C. Zhang, and P. Zoller, Phys. Rev. Lett. **98**, 010506 (2007).
[31] V. Gurarie and L. Radzihovsky, Phys. Rev. B **75**, 212509 (2007).
[32] T. Mizushima, M. Ichioka, and K. Machida, Phys. Rev. Lett. **101**, 150409 (2008).
[33] Y. Tsutsumi, T. Kawakami, T. Mizushima, M. Ichioka, and K. Machida, Phys. Rev. Lett. **101**, 135302 (2008).
[34] H. Mäkelä, Y. Zhang, and K.-A. Suominen, J. Phys. A **36**, 8555 (2003).
[35] H. Mäkelä, J. Phys. A **39**, 7423 (2006).
[36] G. W. Semenoff and F. Zhou, Phys. Rev. Lett. **98**, 100401 (2007).
[37] M. Kobayashi, Y. Kawaguchi, M. Nitta, and M. Ueda, Phys. Rev. Lett. **103**, 115301 (2009).
[38] B. Lian, T.-L. Ho, and H. Zhai, Phys. Rev. A **85**, 051606(R) (2012).
[39] S. Kobayashi, N. Tarantino, and M. Ueda, Phys. Rev. A **89**, 033603 (2014).

[40] J. Preskill, Lecture notes for physics 219: Quantum computation, http://www.theory.caltech.edu/~preskill/ph219/topological.pdf, 2004 (to be published).

[41] J. Schwinger, Phys. Rev. **144,** 1087 (1966).

[42] J. Schwinger, Phys. Rev. **173,** 1536 (1968).

[43] D. Zwanziger, Phys. Rev. **176,** 1489 (1968).

[44] E. Witten, Phys. Lett. **86B,** 283 (1979).

[45] M. de Wild Propitius and F. A. Bais, in *Particles and Fields*, edited by G. Semenoff and L. Vinet, CRM Series in Mathematical Physics (Springer Verlag, New York, 1998), p. 353.

[46] M. G. Alford, K. Benson, S. Coleman, J. March-Russell, and F. Wilczek, Phys. Rev. Lett. **64,** 1632 (1990).

[47] J. Preskill and L. M. Krauss, Nucl. Phys. **B341,** 50 (1990).

[48] K. O. Roberts, T. McKellar, J. Fekete, A. Rakonjac, A. B. Deb, and N. Kjærgaard, Opt. Lett. **39,** 2012 (2014).

[49] E. C. Samson, K. E. Wilson, Z. L. Newman, and B. P. Anderson, Phys. Rev. A **93,** 023603 (2016).

[50] C. V. Ciobanu, S.-K. Yip, and T.-L. Ho, Phys. Rev. A **61,** 033607 (2000).

[51] J. A. M. Huhtamäki, T. P. Simula, M. Kobayashi, and K. Machida, Phys. Rev. A **80,** 051601(R) (2009).

[52] Y. Kawaguchi and M. Ueda, Phys. Rep. **520,** 253 (2012).

[53] M. O. Borgh and J. Ruostekoski, Phys. Rev. Lett. **117,** 275302 (2016).

[54] T. Mawson, T. C. Petersen, and T. Simula, Phys. Rev. A **96,** 033623 (2017).

[55] See Supplemental Material at http://link.aps.org/supplemental/10.1103/PhysRevLett.123.140404 for supporting theoretical and numerical details, movies, and figures, which includes Refs. [56–75].

[56] N. N. Klausen, J. L. Bohn, and C. H. Greene, Phys. Rev. A **64,** 053602 (2001).

[57] H. Schmaljohann, M. Erhard, J. Kronjäger, M. Kottke, S. van Staa, L. Cacciapuoti, J. J. Arlt, K. Bongs, and K. Sengstock, Phys. Rev. Lett. **92,** 040402 (2004).

[58] A. Widera, F. Gerbier, S. Fölling, T. Gericke, O. Mandel, and I. Bloch, New J. Phys. **8,** 152 (2006).

[59] Y. Kawaguchi and M. Ueda, Phys. Rev. A **84,** 053616 (2011).

[60] R. Barnett, A. Turner, and E. Demler, Phys. Rev. A **76,** 013605 (2007).

[61] S.-K. Yip, Phys. Rev. A **75,** 023625 (2007).

[62] H. Mäkelä and K.-A. Suominen, Phys. Rev. Lett. **99,** 190408 (2007).

[63] M. Fizia and K. Sacha, J. Phys. A **45,** 045103 (2012).

[64] L. Carroll and S. M. Wiggins, *Alice's Adventures in Wonderland* (Collins, Sydney, 1983), p. 143.

[65] T. P. Simula, T. Mizushima, and K. Machida, Phys. Rev. Lett. **101,** 020402 (2008).

[66] T. H. Koornwinder, B. J. Schroers, J. K. Slingerland, and F. A. Bais, J. Phys. A **32,** 8539 (1999).

[67] C. Mochon, Phys. Rev. A **67,** 022315 (2003).

[68] L. DiCarlo, J. M. Chow, J. M. Gambetta, Lev S. Bishop, B. R. Johnson, D. I. Schuster, J. Majer, A. Blais, L. Frunzio, S. M. Girvin, and R. J. Schoelkopf, Nature (London) **460,** 240 (2009).

[69] G. Gauthier, I. Lenton, N. M. Parry, M. Baker, M. J. Davis, H. Rubinsztein-Dunlop, and T. W. Neely, Optica **3,** 1136 (2016).

[70] J. Dalibard, F. Gerbier, G. Juzeliūnas, and P. Öhberg, Rev. Mod. Phys. **83,** 1523 (2011).

[71] A. Farolfi, D. Trypogeorgos, G. Colzi, E. Fava, G. Lamporesi, and G. Ferrari, arXiv:1907.06457.

[72] K. Aikawa, A. Frisch, M. Mark, S. Baier, A. Rietzler, R. Grimm, and F. Ferlaino, Phys. Rev. Lett. **108,** 210401 (2012).

[73] G. R. Dennis, J. J. Hope, and M. T. Johnsson, Comput. Phys. Commun. **184,** 201 (2013).

[74] T. P. Simula, P. Engels, I. Coddington, V. Schweikhard, E. A. Cornell, and R. J. Ballagh, Phys. Rev. Lett. **94,** 080404 (2005).

[75] M. Kobayashi (private communication).

[76] J. Ruostekoski and J. R. Anglin, Phys. Rev. Lett. **86,** 3934 (2001).

[77] C. Mochon, Phys. Rev. A **69,** 032306 (2004).

[78] H. M. Hurst and I. B. Spielman, Phys. Rev. A **99,** 053612 (2019).

[79] T. Simula, Phys. Rev. A **97,** 023609 (2018).

[80] S. M. M. Virtanen, T. P. Simula, and M. M. Salomaa, Phys. Rev. Lett. **87,** 230403 (2001).

[81] N. Goldman, G. Juzeliūnas, P. Öhberg, and I. B. Spielman, Rep. Prog. Phys. **77,** 126401 (2014).

[82] S. Sugawa, F. Salces-Carcoba, A. R. Perry, Y. Yue, and I. B. Spielman, Science **360,** 1429 (2018).